Separation of Lithium from Ores in Seconds

Shichen Xu,[1,#] Justin Sharp,[1,#] Alex Lathem,[1,2] Qiming Liu,[1] Lucas Eddy,[1,2] Shihui Chen,[1] Bowen Li,[1] Tengda Si,[1] Jaeho Shin,[1] Chi Hun Choi,[3] Yimo Han,[3] Boris I. Yakobson,[1,2,3,4] Yufeng Zhao,[3,5*] and James M. Tour[1,2,3,4*]

[1]Department of Chemistry, Rice University, Houston TX, 77005, USA.

[2]Applied Physics Program and Smalley-Curl Institute, Rice University, Houston TX, 77005, USA.

[3]Department of Materials Science and NanoEngineering, Rice University, Houston TX, 77005, USA.

[4]NanoCarbon Center and the Rice Advanced Materials Institute, Rice University, Houston TX, 77005, USA.

[5]Department of Physics, Corban University, 5000 Deer Park Drive SE, Salem, OR 97317, USA.

[#] Those authors contributed equally: Shichen Xu, Justin Sharp

* Corresponding authors: J.M.T. (tour@rice.edu), Y.Z. (yz173@rice.edu)

Abstract Lithium (Li) is the lowest density metal, and therefore an optimal element in most battery designs[1,2]. With the increasing demand for Li, metallurgical techniques using excess acid leaching of mineral ores are common. However, these techniques are limited by complex, multi-step processes with adverse environmental impacts caused by secondary waste streams[1,3]. Here, we show that flash Joule heating (FJH) can convert the earth-abundant Li ore, α-spodumene, into β-spodumene in seconds, making LiCl extractable with 1 M HCl (Method A). Even more simply, we

show that a one-step FJH of α-spodumene under an atmosphere of Cl_2 (FJH-Cl_2) can afford high-purity and high-yield LiCl in seconds without any acid treatment (Method B). This capitalizes upon the lower ΔG_{form} of the LiCl over the competing aluminum and silicon chlorides. Spodumene undergoes the FJH-Cl_2 reaction at 1550 °C in seconds, whereupon LiCl immediately distills from the remaining non-volatile aluminum oxide and silicon oxide. LiCl with a 96% purity and 94% yield can be achieved in this rapid one-step process, enormously reducing costs and waste emissions. Local processing with FJH-Cl_2 can dramatically lessen the complexity and cost in obtaining Li, obviating remote mining, and facilitating the world's progression toward cleaner renewable energies[2,3].

Introduction

Li is an essential component in lithium-ion and lithium-metal batteries, which account for most portable renewable energy storage systems, and the drivers of the ubiquitous internet of things and electric vehicles[1,2]. This has led to a global surge in Li demand[4]. The supply of Li, however, is confronted with obstacles, including a lack of raw materials, the need for remote mining, environmental concerns, and the complexity of Li extraction and separation[1,3]. Efficient separation of Li is crucial to prevent supply chain disruptions and to minimize secondary waste streams, while economically incentivizing the mining industry[5,6]. Primary natural sources of Li are in brine deposits and mineral ores[7-9]. Two thirds of Li that is processed worldwide is extracted from brines even though the separation process is slow, and brines have low Li concentrations of

only 1 to 2 wt%. This also requires extensive leaching and months- or years-long evaporation times in ponds that require massive land areas[9,10]. Conversely, Li ores such as spodumene, lithium aluminum inosilicate, $LiAl(SiO_3)_2$, have double the Li content of brines, reaching ~4 wt% of the complex, and ~8 wt% of the total metal content in the ore. However, only one third of Li that is obtained worldwide is extracted from spodumene because of the increased complexity in isolation using this ore instead of brines[8,11-13]. Many wet strategies, including froth flotation[14-16], sulfation[17-21], chlorination[22, 23], carbonation[11,24,25], and fluorination roasting[26,27], have been used to separate Li from spodumene. Among them, the sulfation process has been the standard method for Li separation from mineral ores including spodumene, but sulfation requires extended heating cycles up to 1,100 °C, excess sulfuric acid, and several chemical additives, while generating cumbersome secondary waste streams[17-21].

Flash Joule heating (FJH) is an ultrafast, controllable, and energy-efficient method that has been used for materials synthesis[28-30], waste upcycling[31-33], and recovery of metals[34,35]. We show here that FJH allows spodumene to be converted from its α-phase to its β-phase in high yield in seconds, and LiCl separation can ensue using only 1 M HCl (Method A). However, this method still requires the use of dilute acid. Conversely, we can combine FJH with a gas chlorination process (FJH-Cl_2) as an alternative method of Li separation (Method B). FJH-Cl_2 requires no secondary acid for LiCl separation, and it reduces the processing time to seconds from the days needed in sulfation, and months or more needed when processing Li brines.

Arc welder FJH apparatus

Fig. 1a shows the schematic diagram of the FJH-Cl_2 reaction apparatus. A quartz tube serves as the reaction chamber, while two graphite rods are attached to graphite blocks on either end of a sheet of carbon paper. When chlorine gas (Cl_2) enters the chamber, Li from the spodumene reacts with the Cl_2 to form volatile LiCl that condenses on the inner wall of the quartz tube. The unreacted silicon oxide (SiO_2) and aluminum oxide (Al_2O_3) in the spodumene remain in the residue on the carbon paper, thereby achieving the Li separation. LiCl in the volatile phase can be recovered by rinsing the quartz tube with water. The commercial arc welder used to power this system costs only $125 (Supplementary Fig. S1) and has a maximum power output of 5.8 kW, providing a rapid and stable electrical heat source for the reaction.

The first advantage of this setup is temperature controllability, achieved by adjusting the current setting on the arc welder dial (Fig. 1b). The temperature profile of the carbon paper was measured using an infrared thermometer, where the temperature was ~1150 °C at a current output setting of 10, and ~1630 ºC at a current setting of 20. The second advantage of this system is temperature uniformity. The surface of the heated carbon paper displays a uniform orange-red color, confirming a uniform temperature induced by FJH across the carbon paper as verified with an infrared thermometer (Fig. 1c and Supplementary Fig. S2). The third advantage is temperature stability. When the current setting is 15, the output current remains steady during the spodumene treatment with Cl_2. The surface temperature of the carbon paper remains at 1420 ºC for the duration of the reaction, emphasizing the temperature stability of this apparatus (Fig. 1d).

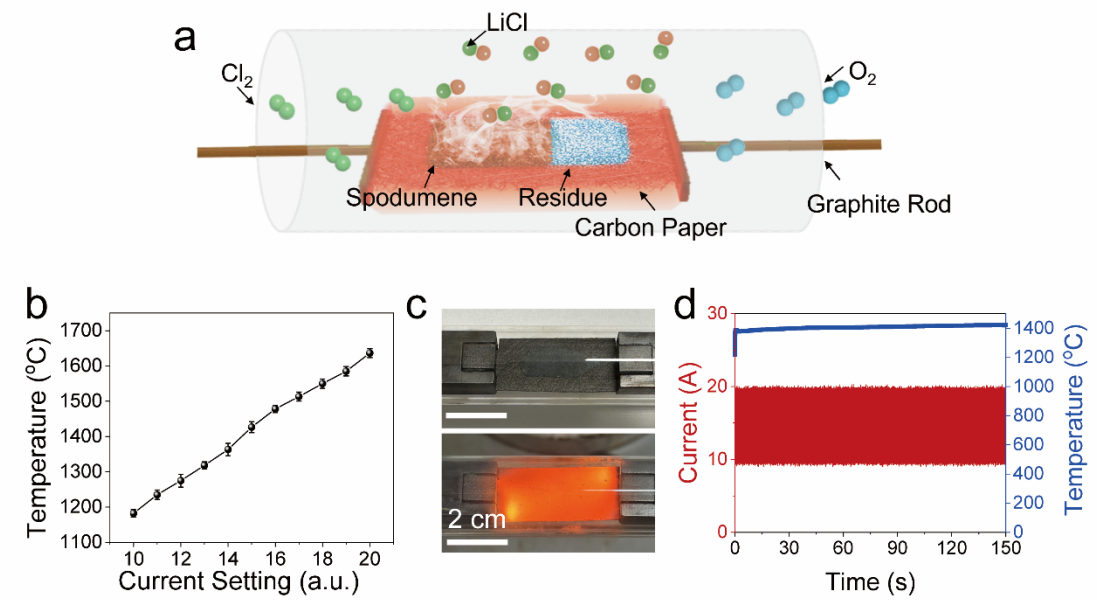

Fig. 1. FJH-Cl_2 for separation and recovery of Li. (a) Schematic diagram of FJH-Cl_2 process, where spodumene is placed on the carbon paper and reacts with Cl_2. Generated LiCl evaporates and condenses on the inside of the quartz tube while the unreacted silicon and aluminum oxide residues remains on the carbon paper. (b) Temperature plot under increasing current settings from 10 to 20. (c) Pictures of carbon paper before (upper) and during (lower) FJH. (d) Real-time temperature (blue) and current (red) with a current setting of 15 for 150 s.

Conversion of α-spodumene to β-spodumene

Spodumene exists in different crystalline phases, typically in its natural α-phase or rock form (Fig. 2a). Before the FJH process, the spodumene rock was ground into micron-sized powder using a mortar and pestle and then sieved through successive meshes with pore sizes of 1000 μm, 200 μm, and 53 μm to obtain particles of corresponding sizes. Scanning electron microscopy (SEM)

images show these particles as uniformly sized but irregularly shaped (Fig. 2a and Supplementary Fig. S3). When spodumene particles are subjected to FJH, the α-phase converts to the β-phase. The X-ray diffraction (XRD) pattern shows that the two phases are clearly different (Fig. 2b and Supplementary Fig. S4)[36]. However, the phase transformation varies with different particle sizes. When using 30 s of FJH at 1150 ºC, signals of the α-phase are still detected in the FJH-treated 200 µm spodumene. There is a strong signal peak at 21.1º, 30.5º, and 32.0º in the XRD pattern, indicating an incomplete phase conversion (Supplementary Fig. S4). Under the same treatment parameters for the 53 µm sample, only the β-phase signal can be found after treatment by FJH (Fig. 2b), revealing that smaller particles are necessary to achieve a complete phase transformation. Raman spectroscopy further illustrates that the untreated α-phase exhibits typical Raman peaks ~370 cm^{-1} and 700 cm^{-1}. The samples treated by FJH only show the characteristic Raman peak of the β-phase at ~500 cm^{-1} (Fig. 2c)[37, 38]. However, using FJH in conjunction with decreasing particle size has a greater effect on improving the LiCl yield than the purity. When the spodumene size is 1000 µm, the yield was improved from 16.3% to 36.8% after FJH, while using 53 µm particles increased the yield from 57% before FJH to 92% after FJH (Fig. 2d). The results of the HCl washing of the LiCl from this phase-converted sample (Method A, Supplementary Fig. S6 and Fig. S7) are described in the Supplementary Text S1.

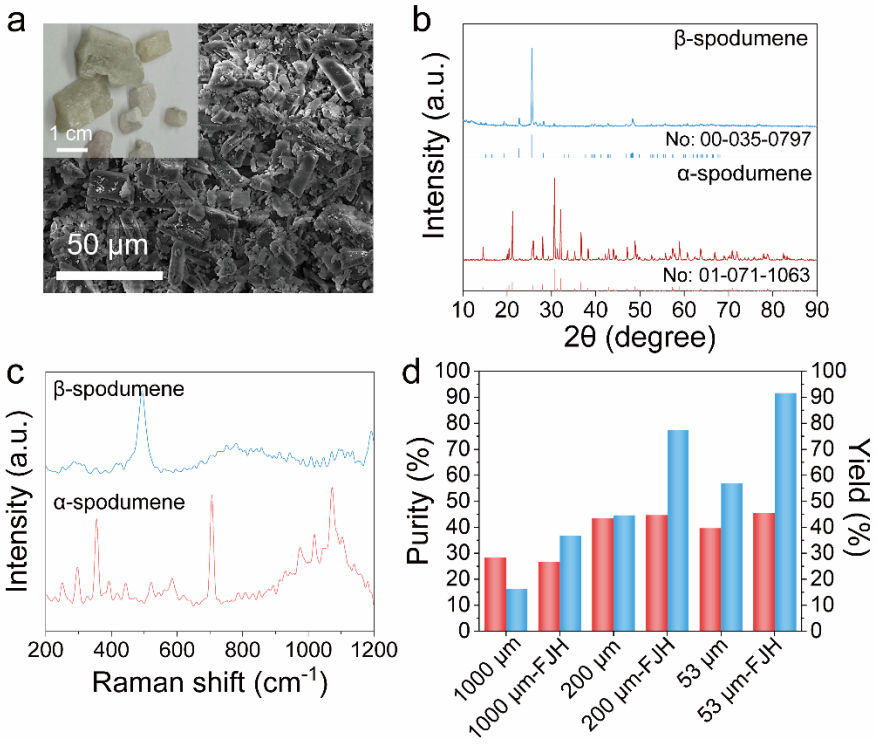

Fig. 2. Phase transformation of spodumene. (a) SEM image of ground spodumene powder with a particle size of 53 μm. The inset image is of the raw α-spodumene sample as received. (b) XRD pattern and (c) Raman spectra of the spodumene before and after phase transformation, where the α-phase (red) is present before heating and the β-phase (blue) is present after FJH at 1150 ºC. (d) The purity (red) and yield (blue) of Li extracted from spodumene using Method A (1 M HCl) with different particle sizes after FJH treatment at 1150 ºC.

FJH-Cl_2 of spodumene

Rapid FJH can achieve the formation of β-spodumene, which is necessary to increase the efficiency of Li extraction. However, this cannot eliminate the use of acid, nor does it overcome the limitations in purity of Li. Therefore, exploring the chemical reactivity of different elements in

spodumene is necessary to achieve efficient Li separation. Inductively coupled plasma mass spectrometry (ICP-MS) results show that the main elements in the purchased spodumene rock are Li, Al, and Si (Fig. 3a). This is consistent with scanning electron microscopy with energy dispersive X-ray spectroscopy (SEM-EDX) (Supplementary Fig. S8) and XPS (Supplementary Fig. S9) results, where the Li content is 4.8%. We conducted a thermodynamic analysis for chlorinating silicon oxide (SiO_2), aluminum oxide (Al_2O_3), and lithium oxide (Li_2O) in α-spodumene. According to the Gibbs free energy change (ΔG) vs. temperature, only Li_2O is chlorinated below 2000 ºC, and chlorination is unfeasible for SiO_2 and Al_2O_3 within that temperature range (Fig. 3b). ΔG is negative for Li_2O when the temperature is higher than 514 ºC, suggesting that Li in spodumene can be chlorinated at ~514 ºC. However, when the chlorination reaction occurs between 514 °C and the boiling point of LiCl (1382 °C), leaching the formed LiCl with water results in low purity and yield of Li due to the interference of Si impurities in the sample (Supplementary Fig. S10). However, when the control temperature is above the boiling point of LiCl, and below 2000 ºC, LiCl can be cleanly volatilized and separated from spodumene (Method B, Supplementary Fig. S5).

When the arc welder settings are 15 and 18, the corresponding temperatures are 1420 ºC and 1550 ºC, respectively. After 30 s of chlorinating spodumene, volatile LiCl deposits on the inner surface of the quartz tube (Fig. 3c). SEM-EDX characterization results indicate that the primary element in the volatile fraction is Cl, with trace amounts of Si and Al (Supplementary Fig. 11a); Li is too light to be detected. XPS results also show that the main elements in the volatile fraction

are Cl, O, and Li (Supplementary Fig. 11b, c). After the chlorination reaction, a significant amount of residue remains on the carbon paper. SEM-EDX results reveal that the main elements in the residue are Si, Al, O, and Cl (Supplementary Fig. 12a), which is consistent with the XPS results (Supplementary Fig. 12b). By comparing the XPS fine spectra of Li in the original spodumene sample with the residue, there is no detectable Li signal in the residue after FJH-Cl_2 (Fig. 3d). This result suggests that the FJH-Cl_2 reaction can selectively and efficiently separate Li as LiCl directly from raw spodumene.

High-temperature vapor-phase reactions can inevitably introduce SiO_2 and Al_2O_3 into the volatile phase via physical mass transport processes during the rapid LiCl volatilization; in an industrialized process, further fractionation plates would be desired. Interestingly, ICP-MS results show that purity can be enhanced when the volatile obtained from the chlorination reaction is rinsed with water (Fig. 3e). LiCl is water-soluble while SiO_2 and Al_2O_3 are not, so the water-wash acts as an additional purification step while extracting only the condensed LiCl from the quartz tube. Additionally, as the particle size of spodumene decreases, the purity of Li increases. When the particle size of spodumene is 53 μm, the purity of Li obtained from FJH-Cl_2 can reach 95% (Fig. 3e). Furthermore, the yield of LiCl is related to the particle size of the sample and the chlorination temperature. When the particle size is 200 μm and the arc welder setting is 15 (1420 ºC), the purity of Li obtained from the FJH-Cl_2 is 88%, but the yield is only 41% (Fig. 3f). Even when the particle size is 53 μm, the yield is still only 64%. However, when the current dial is set to 18 (1550 ºC), and 53 μm spodumene particles are used, extracted LiCl with 96% purity and 94%

yield can be obtained (Fig. 3f). Hence, when the temperature is set to 1550 °C, the LiCl rapidly forms (~512 °C) and distills from the mixture since the LiCl boiling point is 1382 °C. Other sources of spodumene ore were used to ensure that the process worked equally well regardless of the region from which the sample was mined (Supplementary Text S2, Fig. S13 and Fig. S14).

Although the Li process here was only on a laboratory scale, FJH has recently been demonstrated on the 1-tonne day^{-1} production scale for the conversion of inexpensive coal or coke into graphene at ~3000 °C,[40] a temperature nearly twice that needed for LiCl separation. Hence, these approaches can be scaled, thereby serving as a harbinger for the commercializing of this Li separation process.

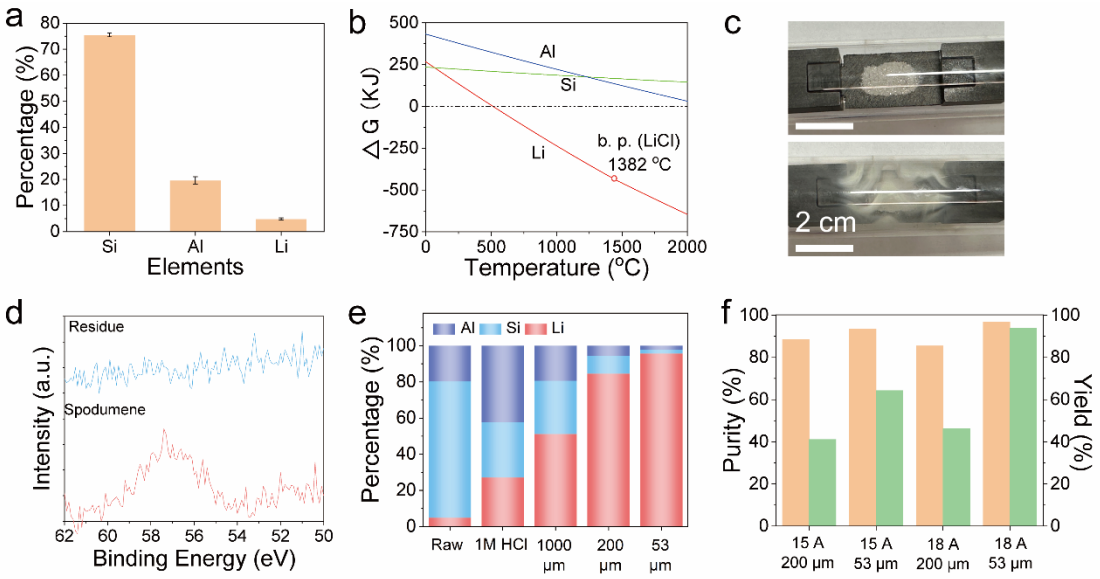

Fig. 3. Separation and recovery of Li from spodumene by FJH-Cl_2. (a) The ICP-MS results of the raw spodumene. (b) Thermodynamic analysis of the chlorination reaction of the metal oxides. Only the chlorination of Li_2O is feasible above 514 ºC when the ΔG is negative (below the black dotted line). (c)

Picture of quartz tube containing spodumene before (upper) and after (lower) FJH-Cl_2 when the LiCl (white volatile) has condensed inside the quartz tube. (d) XPS spectra of spodumene before (red) and residue after (blue) FJH-Cl_2. The Li 1s signal is only detected before FJH-Cl_2. (e) The composition of Li, Si, and Al in raw spodumene, after FJH-Cl_2 below the boiling point of LiCl followed by acid washing, and the volatile phase after FJH-Cl_2 above the boiling point of LiCl, shown for each of the three particle sizes. (f) The purity (orange) and yield (green) of LiCl after FJH-Cl_2 of spodumene at current settings of 15 (1420 ºC) and 18 (1550 ºC) for 30 s each.

Density Functional Theory Calculations

To understand why the chlorination method can so efficiently and quickly separate Li from spodumene, density functional theory (DFT) calculations were employed to further explore the mechanism of this process. The energy required to separate 50% and 100% of the Li from both α-spodumene and β-spodumene between 1600 K and 2000 K and at 1, 6, and 11 atm was calculated (Fig. 4, Supplementary Fig. 15 and 16). Generally, natural spodumene is in the α-phase, which is monoclinic (Fig. 4a and Supplementary Fig. 15a), after extracting all the Li, the structure is different from the α-phase spodumene but still stable (Fig. 4b and Supplementary Fig. 15b). When increasing the temperature from 1600 K to 2000 K and decreasing the pressure from 11 atm to 1 atm, the chlorination for extracting Li from α-phase spodumene requires less energy (Fig. 4c). During the FJH process, the spodumene readily converts from the monoclinic α-phase to the tetragonal β-phase (Fig. 4d and Supplementary Fig. 15c). After extracting the Li from β-phase

spodumene, the structure frame (Fig. 4e and Supplementary Fig. 15d) is totally different from that of α-phase spodumene. More importantly, delithiation from the β-phase spodumene requires less energy under the same temperature and pressure than the α-phase. Full delithiation energy from β-phase spodumene is by 0.15 eV/Li lower than that of α-phase spodumene (Fig. 4f), and by 0.26 eV/Li lower than α-phase spodumene for half delithiation (Supplementary Fig. S16). These results show that delithiation of β-phase spodumene is significantly more exothermic and therefore more favorable than α-phase spodumene. This indicates that during the FJH-Cl_2 process, spodumene first converts from the α-phase to the β-phase before reacting with Cl_2 allowing for a lower- energy Li separation process.

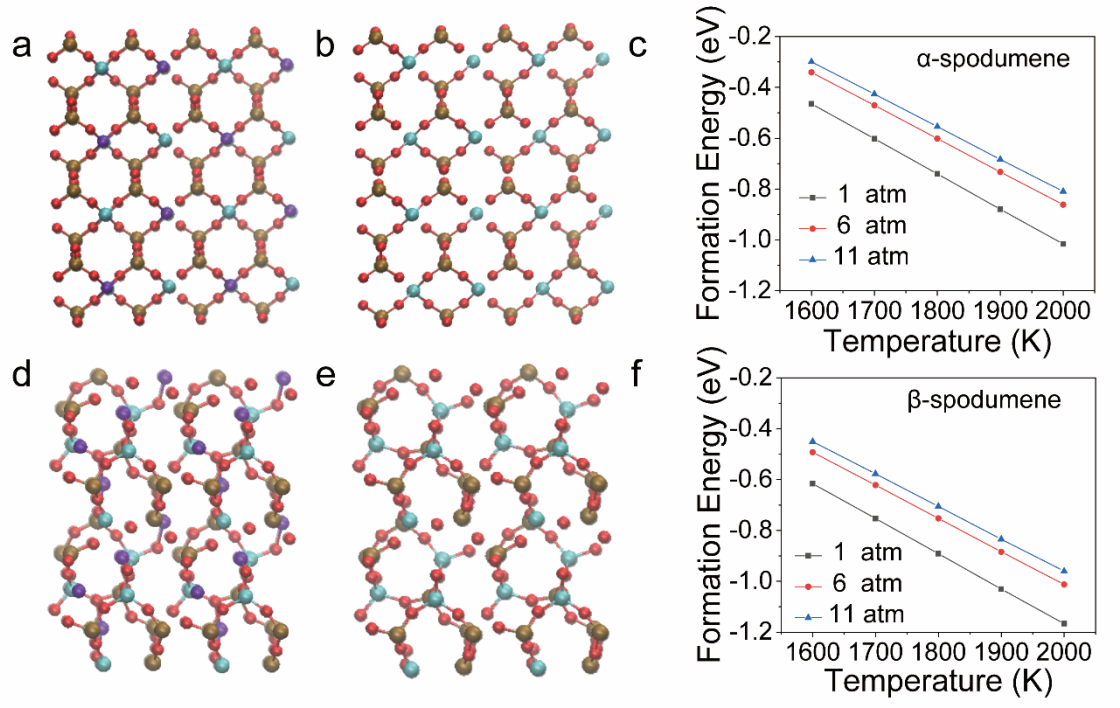

Fig. 4. DFT results for the delithiation energy of α-phase and β-phase spodumene. Top-view ball and stick model of α-phase spodumene before (a) and after (b) extracting 100% of Li. Red: O atoms; cyan: Al atoms; brown: Si atoms; violet: Li atoms. (c) Formation energy (Gibbs free energy) of delithiated α-phase spodumene at various temperatures and pressures. Top-view ball and stick model of β-phase spodumene before (d) and after (e) extracting 100% of Li. (f) Formation energy of delithiated β-phase spodumene at various temperatures and pressures.

LCA, TEA, and environmental impacts

A Monte Carlo life cycle assessment (LCA) and techno-economic analysis (TEA) were employed, and the details are explained in the Supplementary Text S3. The primary factors considered were energy consumption, greenhouse gas emissions of CO_2 listed as global warming potential (GWP), water and acid consumption, and processing cost (Fig. 5). These factors were chosen since they contribute the most to materials costs, consumption, and produced waste. Processing 1 tonne of high-grade spodumene ore produces 44 to 48 kg of Li for both methods because similar yields are achieved in both FJH-Cl_2 and sulfation processes. The LCA shows that FJH-Cl_2 can reduce the process energy consumption by 86% from 15,700 MJ to 2,200 MJ (Fig. 5a), water consumption by 67% from 373,000 kg to 125,000 kg and acid consumption by 100% (Fig. 5d). When accounting for intercontinental transportation in the sulfation process, FJH-Cl_2 can also reduce the GWP by up to 56% from 30,400 kg CO_2 to 13,400 kg CO_2 (Fig. 5b), and the TEA shows a reduction in operating costs of up to 73% from $352,500 to $95,600 (Fig. 5c-d).

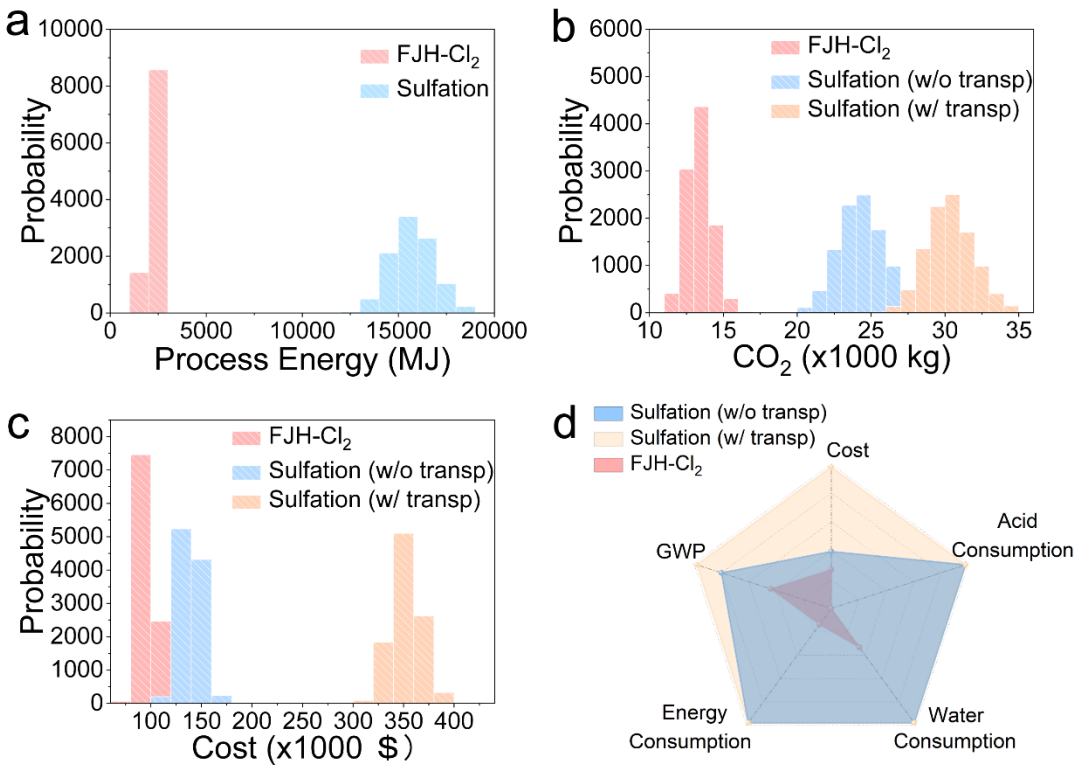

Fig. 5. LCA and TEA results for Li separation by sulfation vs. FJH-Cl_2 with (w/) or without (w/o) intercontinental transportation (transp). Probability histograms for the (a) energy consumption in MJ, (b) GWP in kg CO_2, and (c) processing cost in US dollars necessary to produce 1 tonne of Li. The higher the probability and narrower the plotted histogram, the more accurate the prediction. (d) A radar plot simultaneously comparing the five key variables associated with the FJH-Cl_2 and industrial sulfation processes to produce equal quantities of Li.

Conclusion

Spodumene can be converted from the α-phase to the β-phase with only 30 s of FJH. An inexpensive arc welder can be used on a laboratory scale to facilitate this process. In Method A,

91% yield of the Li is extracted from spodumene using FJH and 1 M HCl. In Method B shows a FJH-Cl_2 method to separate Li with 96% purity and a 94% yield. DFT calculations indicate that extracting Li from β-phase spodumene requires less energy, suggesting that spodumene converts first from the α-phase to the β-phase during the chlorination. LCA and TEA confirmed that the acid-free FJH-Cl_2 method can greatly reduce the total energy consumption, capital and operating costs, water consumption and emissions compared to the industrial standard, sulfuric acid leaching. Capitalizing upon the differences in ΔG_{form} of the LiCl vs. silicon and aluminum chlorides, these results showcase the FJH-Cl_2 method as an efficient and environmentally friendly process for Li separation from ores. The process will likely extend into the separation of Li from spent batteries, and other metals in electronic wastes[41]. This rapid Li separation method permits local Li assets to be developed, lessening costs for renewable energy transitions.

Materials and methods

Materials. The carbon paper was purchased from FuelCellStore (Toray Carbon Paper 060). Bulk spodumene crystals were purchased from EmpathMoonGems (Bulk Kunzite Spodumene Crystals) which are normally sourced from one of four locations: Afghanistan, Brazil, United States or Madagascar[42]. The spodumene sand was received from Australia. Both spodumene samples were ground into micron-sized powder using a mortar and pestle and then sieved through meshes with pore sizes of 1000 μm, 200 μm, and 53 μm to obtain particles of corresponding sizes. Nitric acid (HNO_3, 67-70 wt%, TraceMetal™ Grade, Fisher Chemical), hydrochloric acid (HCl, 37 wt%,

99.99%, trace metal basis, Millipore Sigma), hydrofluoric acid (HF, 48 wt%, 99.99%, trace metal grade for ICP analysis, Millipore Sigma), and ultrapure water (Millipore Sigma, ACS reagent for ultra-trace analysis) were used for sample digestion. A Cl_2 cylinder (Millipore Sigma, 99.5%, 85 psi, 454 g) was used to supply the Cl_2. Argon gas (Airgas, 99.99%) was used to purge the system to remove moisture and air in the reaction chamber prior to the introduction of Cl_2. The arc welder power supply used as a DEKOPRO DKUS-MMA-160A arc welder (Amazon, $120)[43]. The arc welder displays a "current" setting on the screen ranging from 8-160. While the arc welder dial settings correspond to increasing current as they are turned higher, they are not an absolute current setting in amperes that matches with the dial setting number. The details of the FJH and FJH-Cl_2 system have been described previously[41].

Joule heating chlorination system. The Joule heating system comprises a power source, graphite rod, graphite block, and carbon paper. The power source here is the commercial arc welder, connected to the carbon paper via graphite rods and graphite blocks. The temperature of the carbon paper was measured using a Micro-Epsilon thermometer, CTM-3SF75H2-C and CTRM-1H1SF100-C3. The former tests the temperature range between 200-1500 ºC, and the latter tests the temperature range between 1500-3000 ºC. The spodumene sample (50 mg) is spread evenly on the surface of carbon paper in a quartz tube and sealed at the ends of the tube with electrodes, an inlet chlorine gas line, and an outlet volatile gas line for unreacted chlorine. The quartz tube is conventionally 2.54 cm in interior diameter and 20 cm long. The size of carbon paper is usually 2 x 6 cm, and the resistance is 0.8-1.0 Ω. Argon gas (Airgas, 99.99%) is initially introduced into the

chamber to purge the system atmosphere combined with a pumping system, and then chlorine gas (Millipore Sigma, 99.5%) is introduced into the reaction system. Connected to the outlet of the reaction system is a sodium hydroxide bath, which absorbs the unreacted chlorine gas.

Characterization. XRD was performed by the Rigaku SmartLab system with filtered Cu Kα radiation (λ = 1.5406 Å). Raman spectra were acquired using a Renishaw Raman microscope (laser wavelength of 532 nm, laser power of 5 mW, 50 × lens). SEM images were obtained using a FEI Quanta 400 ESEM FEG system at 20 kV. EDS spectra and maps were acquired using the same system equipped with an EDS detector. XPS was conducted using a PHI Quantera XPS system at a base pressure of 5×10^{-9} Torr. Elemental spectra were obtained with a step size of 0.1 eV with a pass energy of 26 eV. All the XPS spectra were calibrated using the standard C 1*s* peak at 284.8 eV.

ICP-MS measurement. Total digestion is used to analyze the element content in raw spodumene. 50 mg of samples with a size of ~1000 μm diameter were dissolved in 5 mL solution of hydrochloric acid (HCl, 37 wt%, 99.99%, trace metal basis, Millipore Sigma), nitric acid (HNO_3, 67-70 wt%, TraceMetal™ Grade, Fisher Chemical), and hydrofluoric acid (HF, 48 wt%, 99.99%, trace metal grade for ICP analysis, Millipore Sigma) with a volume ratio of 3:1:1 and placed in an ultrasonic bath for 12 h. The leaching experiment uses 30 mg of unreacted spodumene powder and 30 mg of FJH-treated powder in 5 mL of 1 M HCl for 6 h. Here, the leaching rates of Li were compared not only for samples with the same particle size but also for leaching temperatures at both room temperature (22 ºC) and 90 ºC. For testing the volatile phase, the samples washed with

DI water are collected first, and then the supernatant is dissolved in 2 wt % dilute HNO_3, which is then diluted to target concentrations for ICP-MS testing. The Periodic Table mix 1 (Millipore Sigma, 33 elements of Al, As, Ba, Be, Bi, B, Ca, Cd, Cs, Cr, Co, Cu, Ga, In, Fe, Pb, Li, Mg, Mn, Ni, P, K, Rb, Se, Si, Ag, Na, Sr, S, Te, Tl, V, and Zn, 10 mg L^{-1} each, in 10 wt % HNO_3 containing HF traces) and Periodic Table mix 2 (Millipore Sigma, 17 elements of Au, Ge, Hf, Ir, Mo, Nb, Pd, Pt, Re, Rh, Ru, Sb, Sn, Ta, Ti, W, and Zr, 10 mg L^{-1} each, in 5% HF and 1% HCl containing HNO_3 traces) were used as the standard solution.

DFT computational methods.

We perform density-functional-theory (DFT)[44] modeling of FJH-Cl_2 delithiation of spodumene ($LiAlSi_2O_6$) as expressed in the following reaction:

$$LiAlSi_2O_6 + (x/2)\ Cl_2 = x\ LiCl + Li_{(1-x)}AlSi_2O_6, \quad (1)$$

Where x = 0.5 and 1.0, respectively, for 50% and 100% of Li atoms being extracted out of spodumene. The Gibbs free energy (formation energy) of the reaction can be calculated following the equation:

$$G = [E_{\text{products}} - E_{\text{reactants}} + x\mu_{\text{LiCl}} - \left(\frac{x}{2}\right)\mu_{Cl_2}]/x, \quad (2)$$

where E_{products} and $E_{\text{reactants}}$ are the DFT total energy of all products and reactants according to their chemical formula and stoichiometric ratio, and μ_{Cl_2} and μ_{LiCl} are the chemical potentials of Cl_2 and LiCl in gas phase. The chemical potential of Cl_2 gas as a function of pressure p and temperature T can be calculated following the equation[45]:

$$\mu_{Cl_2}(T,p) = H(T,p^0) - H(0K,p^0) - T[S(T,p^0) - S(0K,p^0)] + kTln(p/p^0), \quad (3)$$

where the $p^0 = 1atm$, and the entropy $S(T, p^0)$, enthalpy $H(T, p^0)$ are taken from the thermochemical tables[46]. For LiCl, the same method is used.

DFT methods are used as they are implemented in the Vienna Ab-initio Simulation Package (VASP)[47]. A plane wave expansion up to 520 eV is employed in combination with an all-electron-like projector augmented wave (PAW) potential[48]. Exchange-correlation is treated within the generalized gradient approximation (GGA) using the functional parameterized by Perdew-Burke-Ernserhof[49]. Periodic condition is applied to the supercell or unit cell of crystal structures, with Brillouin zone integration converges over Monkhorst-Pack type mesh[50]. In structure optimization using the conjugate-gradient algorithm as implemented in VASP, both the positions of atoms and the size of unit cells are fully relaxed so that the maximum force on each atom is smaller than 0.01 eV/Å.

The α- and β-spodumene were modeled in supercells each having 4 Li atoms, 4 Al atoms, 8 Si atom, and 24 O atoms. We found that the overall frameworks of α- and β-spodumene remain to be stable except for slight deformation (see Figs. 2 and 3, and the details of structural coordinates can be found in the data uploaded related to this paper). For the partially delithiated spodumene $Li_{(1-x)}AlSi_2O_6$ (x = 0.5), we search the most energetically favorable structure in all possible configurations in which two of the four Li atoms in the original spodumene were removed. The LiCl has an FCC crystal structure with lattice constant of a = 2.574 Å and the Cl_2 molecule is optimized inside a vacuum box of 20 Å × 20 Å × 20 Å.

LCA and TEA. The TEA and LCA were performed using the OpenLCA software[51]. Monte-Carlo simulations were performed for both processes with 10,000 iterations at a 95% confidence interval for all variables to assess the necessary inputs to produce 1 tonne of Li from the FJH-Cl_2 and industrial sulfation processes. The data used to simulate the industrial spodumene treatment process was collected from the literature to compare with experimental variables for the FJH-Cl_2 process. Data analysis from the Monte-Carlo simulations was performed with Microsoft Excel and Python to plot the histograms and radar plots.

Data availability.

All data of the study is available in the main text and the Supplementary Information. Other relevant data are available from the corresponding authors.

Acknowledgements

The funding of the research was provided by the Defense Advanced Research Projects Agency (HR00112290122, J.M.T.), the Air Force Office of Scientific Research (FA9550-22-1-0526, J.M.T.), and the U.S. Army Corps of Engineers, ERDC (W912HZ-21-2-0050 and W912HZ-24-2-0027, J.M.T., B.I.Y., Y.Z.). Computer resources were provided through the DOE NERSC award (BES-ERCAP0027822, B.I.Y.). The characterization equipment used in this project is partly from the Shared Equipment Authority (SEA) at Rice University. The authors thank Dr. Bo Chen of Rice

University for helpful input with the XPS results and Drs. Christopher Pennington and Tanguy Terlier for developing ICP-MS methods.

Author Contributions

S.C.X., Q.M.L. and J.M.T. conceived the idea. S. C. X. and J. S. built and maintained the FJH system. S.C.X. and J.S. conducted the experiment with the help of Q.M.L., L.E., S.H.C., J.S., C.H.C., B.W.L., and T.D.S. and S.X. conducted all the characterization and analysis. J.S. and A.L. conducted the technoeconomic analysis and life-cycle assessment and analyzed the results. Y.Z. and. B.I.Y. conducted the DFT computations of the phase-structures and thermodynamics trends. S.C.X., J.S., and J.M.T. wrote the manuscript. All aspects of the research were overseen by J.M.T. All authors have discussed the results and given approval to the final version of the manuscript.

Competing interests

Rice University owns intellectual property on the separation of metals from waste and ores, including spodumene, using flash Joule heating with or without concomitant chlorination. Much of this intellectual property has been licensed to a company in which J.M.T. is a shareholder, but he is not an employee, officer, or director in that company. Conflicts of interest are mitigated through disclosure to and compliance with the Rice University Office of Research Integrity. The authors declare no other competing interests.

References

1 Olivetti, E. A., Ceder, G., Gaustad, G. G. & Fu, X. Lithium-ion battery supply chain considerations: Analysis of potential bottlenecks in critical metals. *Joule* **1**, 229-243 (2017).

2 Trahey, L. *et al.* Energy storage emerging: A perspective from the Joint Center for Energy Storage Research. *PNAS* **117**, 12550-12557 (2020).

3 Alessia, A., Alessandro, B., Maria, V. G., Carlos, V. A. & Francesca, B. Challenges for sustainable lithium supply: A critical review. *J. Clean. Prod.* **300** 126954 (2021).

4 Xu, C. *et al.* Future material demand for automotive lithium-based batteries. *Commun. Mater.* **1** 99 (2020).

5 Reck B. K. & Graedel T. E. Challenges in metal recycling. *Science* **337**, 690-695 (2012).

6 Graedel, T. E., Harper, E. M., Nassar, N. T., Nuss, P. & Reck, B. K. Criticality of metals and metalloids. *PNAS* **112**, 4257-4262 (2015).

7 Yang, S., Zhang, F., Ding, H., He, P. & Zhou, H. Lithium metal extraction from seawater. *Joule* **2**, 1648-1651 (2018).

8 Tadesse, B., Makuei, F., Albijanic, B. & Dyer, L. The beneficiation of lithium minerals from hard rock ores: A review. *Miner. Eng.* **131**, 170-184 (2019).

9 Vera, M. L., Torres, W. R., Galli, C. I., Chagnes, A. & Flexer, V. Environmental impact of direct lithium extraction from brines. *Nat. Rev. Earth Env.* **4**, 149-165 (2023).

10 Flexer, V., Baspineiro, C. F. & Galli, C. I. Lithium recovery from brines: A vital raw material for green energies with a potential environmental impact in its mining and processing. *Sci. Total Environ.* **639**, 1188-1204 (2018).

11 Dessemond, C., Lajoie-Leroux, F., Soucy, G., Laroche, N. & Magnan, J. F. Spodumene: The lithium market, resources and processes. *Minerals* **9**, 1-17 (2019).

12 Fosu, A. Y., Kanari, N., Vaughan, J. & Chagnes, A. Literature review and thermodynamic modelling of roasting processes for lithium extraction from spodumene. *Metals* **10** 1312 (2020).

13 Zhou, H., Cao, Z., Ma, B., Wang, C. & Chen, Y. Selective and efficient extraction of lithium from spodumene via nitric acid pressure leaching. *Chem. Eng. Sci.* **287** 119736 (2024).

14 Zhu, G. *et al.* Surface features and flotation behaviors of spodumene as influenced by acid and alkali treatments. *Appl. Surf. Sci.* **507** 145058 (2020).

15 Xie, R., Zhu, Y., Liu, J. & Li, Y. The flotation behavior and adsorption mechanism of a new cationic collector on the separation of spodumene from feldspar and quartz. *Sep. Purif. Technol.* **264** 118445 (2021).

16 Xie, R., Zhu, Y., Liu, J. & Li, Y. Flotation behavior and mechanism of α-bromododecanoic acid as collector on the flotation separation of spodumene from feldspar and quartz. *J. Mol. Liq*. **336** 116303 (2021).

17 Meshram, P., Pandey, B. D. & Mankhand, T. R. Extraction of lithium from primary and secondary sources by pre-treatment, leaching and separation: A comprehensive review. *Hydrometallurgy* **150**, 192-208 (2014).

18 Yan, Q. *et al.* Extraction of valuable metals from lepidolite. *Hydrometallurgy* **117**, 116-118 (2012).

19 Guo, H., Kuang, G., Wang, H., Yu, H. & Zhao, X. Investigation of enhanced leaching of lithium from α-spodumene using hydrofluoric and sulfuric acid. *Minerals* **7** 205 (2017).

20 Kuang, G. *et al.* Extraction of lithium from β-spodumene using sodium sulfate solution. *Hydrometallurgy* **177**, 49-56 (2018).

21 Lajoie-Leroux, F., Dessemond, C., Soucy, G., Laroche, N. & Magnan, J.-F. Impact of the impurities on lithium extraction from β-spodumene in the sulfuric acid process. *Miner. Eng.* **129**, 1-8 (2018).

22 Barbosa, L. I., González, J. A. & Ruiz, M. d. C. Extraction of lithium from β-spodumene using chlorination roasting with calcium chloride. *Thermochim. Acta* **605**, 63-67 (2015).

23 Barbosa, L. I., Valente, G., Orosco, R. P. & González, J. A. Lithium extraction from β-spodumene through chlorination with chlorine gas. *Miner. Eng.* **56**, 29-34 (2014).

24 Chen, Y., Tian, Q., Chen, B., Shi, X. & Liao, T. Preparation of lithium carbonate from spodumene by a sodium carbonate autoclave process. *Hydrometallurgy* **109**, 43-46 (2011).

25 Santos, L. L. d., Nascimento, R. M. d. & Pergher, S. B. C. Beta-spodumene: Na_2CO_3:NaCl system calcination: A kinetic study of the conversion to lithium salt. *Chem. Eng. Res. Des.* **147**, 338-345 (2019).

26 Rosales, G. D., Ruiz, M. d. C. & Rodriguez, M. H. Novel process for the extraction of lithium from β-spodumene by leaching with HF. *Hydrometallurgy* **147-148**, 1-6 (2014).

27 Rosales, G. D., Resentera, A. C. J., Gonzalez, J. A., Wuilloud, R. G. & Rodriguez, M. H. Efficient extraction of lithium from β-spodumene by direct roasting with NaF and leaching. *Chem. Eng. Res. Des.* **150**, 320-326 (2019).

28 Yao, Y. G. *et al.* Carbothermal shock synthesis of high-entropy-alloy nanoparticles. *Science* **359**, 1489-1494 (2018).

29 Zheng, X. *et al.* Hydrogen-substituted graphdiyne-assisted ultrafast sparking synthesis of metastable nanomaterials. *Nat. Nanotechnol.* **18**, 153-159 (2023).

30 Chen, Y. *et al.* Ultra-fast self-assembly and stabilization of reactive nanoparticles in reduced graphene oxide films. *Nat. Commun.* **7**, 12332 (2016).

31 Cheng, Y. *et al.* Flash upcycling of waste glass fibre-reinforced plastics to silicon carbide. *Nat. Suatain.* **7**, 452-462 (2024).

32 Wyss, K. M. *et al.* Upcycling of waste plastic into hybrid carbon nanomaterials. *Adv. Mater.* **35**, e2209621 (2023).

33 Dong, Q. *et al.* Depolymerization of plastics by means of electrified spatiotemporal heating. *Nature* **616**, 488-494 (2023).

34 Chen, W. Y. *et al.* Battery metal recycling by flash Joule heating. *Sci. Adv.* **9**, eadh5131 (2023).

35 Deng, B. *et al.* Rare earth elements from waste. *Sci. Adv.* **8**, eabm3132 (2022).

36 Abdullah, A. A. *et al.* Phase transformation mechanism of spodumene during its calcination. *Miner. Eng.* **140** (2019).

37 Andrei Buzatu, N. B. The Raman study of single-chain silicates. *Analele Stiint. ale Univ.* **4**, 107-125 (2010).

38 Pommier, C. J. S., Denton, M. B. & Downs, R. T. Raman spectroscopic study of spodumene ($LiAlSi_2O_6$) through the pressure-induced phase change from C2/c to P21/c. *J. Raman Spectrosc.* **34**, 769-775 (2003).

39 U.S. Geological Survey, 2024, Mineral commodity summaries 2024: U.S. Geological Survey, 212 p., https://doi.org/10.3133/mcs2024. Accessed 30 Mar. 2024.

40 Universal Matter, https://www.universalmatter.com. Accessed 30 Mar. 2024.

41 Deng, B. *et al*. Flash separation of metals by electrothermal chlorination. Preprint at *https://chemrxiv.org/engage/chemrxiv/article-details/66a1627a01103d79c58aaa83* (2024).

42 Gemological Institute of America Inc., Kunzite Description, https://www.gia.edu/kunzite-description. Accessed 30 Mar. 2024.

43 Eddy L., *et al.* Kilogram flash Joule heating synthesis with an arc welder. Preprint at https://chemrxiv.org/engage/chemrxiv/article-details/66a25d215101a2ffa8053791 (2024).

44 Dudarev S. L., Botton G. A., Savrasov S. Y., Humphreys C. J. & Sutton A. P., Electron-energy-loss spectra and the structural stability of nickel oxide: An LSDA+U study. *Phys. Rev. B* **57**, 1505-1509 (1998).

45 Reuter K. & Scheffler M., Composition, structure, and stability of RuO_2 (110) as a function of oxygen pressure. *Phys. Rev. B* **65**, 035406 (2002).

46 Stull D.R. & Prophet H., JANAF Thermochemical Tables, 2nd ed. ~U.S. National Bureau of Standards, Washington, DC (1971).

47 Kresse G. & Furthmuller J., Efficient iterative schemes for *ab initio* total-energy calculations using a plane-wave basis set. *Phys. Rev. B* **54**, 11169-11186 (1996)

48 Blochl P. E., Projector augmented-wave method. *Phys. Rev. B* **50**, 17953-17979 (1994).

49 Perdew J. Burke P., K., & Ernzerhof M., Generalized gradient approximation made simple. *Phys. Rev. Lett.* **77**, 3865 (1996).

50 Monkhorst H. J. & Pack J. D., Special points for Brillouin-zone integrations. *Phys. Rev. B* **13**, 5188-5192 (1976).

51 OpenLCA software. https://www.openlca.org. Accessed 1 Jun. 2024.